Combining PALM and SOFI for quantitative imaging of focal adhesions in living cells

Hendrik Deschout[a], Tomas Lukes[b,c], Azat Sharipov[b], Lely Feletti[a], Theo Lasser[b], Aleksandra Radenovic*[a]

[a]Laboratory of Nanoscale Biology, EPFL, Station 17, CH-1015 Lausanne, Switzerland; [b]Laboratoire d'Optique Biomédicale, EPFL, Station 17, CH-1015 Lausanne, Switzerland; [c]Department of Radioelectronics, Czech Technical University in Prague, Technicka´ 2, 166 27 Prague 6, Czech Republic

ABSTRACT

Focal adhesions are complicated assemblies of hundreds of proteins that allow cells to sense their extracellular matrix and adhere to it. Although most focal adhesion proteins have been identified, their spatial organization in living cells remains challenging to observe. Photo-activated localization microscopy (PALM) is an interesting technique for this purpose, especially since it allows estimation of molecular parameters such as the number of fluorophores. However, focal adhesions are dynamic entities, requiring a temporal resolution below one minute, which is difficult to achieve with PALM. In order to address this problem, we merged PALM with super-resolution optical fluctuation imaging (SOFI) by applying both techniques to the same data. Since SOFI tolerates an overlap of single molecule images, it can improve the temporal resolution compared to PALM. Moreover, an adaptation called balanced SOFI (bSOFI) allows estimation of molecular parameters, such as the fluorophore density. We therefore performed simulations in order to assess PALM and SOFI for quantitative imaging of dynamic structures. We demonstrated the potential of our PALM–SOFI concept as a quantitative imaging framework by investigating moving focal adhesions in living cells.

Keywords: PALM, SOFI, focal adhesion, quantitative imaging, live cell imaging, super-resolution imaging

1. INTRODUCTION

Cell adhesion is an essential aspect of many cellular processes, such as migration or differentiation[1]. For this purpose, cells rely on thin dynamic structures close to the cell membrane, consisting of transmembrane receptors that bind to the extracellular matrix and recruit other proteins from the cytoplasm. Initially, these structures are smaller than 100 nm, but they can mature into larger micron sized assemblies, involving up to hundreds of different proteins[2]. These mature structures are known as focal adhesions, and can be envisaged as the anchor points of the actin cytoskeleton onto the extracellular matrix. Considering their density and size, it is a difficult task to observe the spatial organization of proteins inside focal adhesions.

Photo-activated localization microscopy (PALM), based on localizing single fluorescent proteins in a sequence of camera frames with a precision in the order of 10 nm, is an interesting method for this purpose[3]. Indeed, assuming that each fluorophore is localized once, PALM could be used to count fluorescent proteins inside focal adhesions. However, fluorescent proteins can switch on and off several times after being activated, a phenomenon known as "blinking"[4]. Several methods have been developed to account for the resulting over-counting error, for instance by combining localizations that are clustered in space and time[5, 6] or by applying pair correlation analysis[7].

However, PALM, and by extension PALM based counting, assumes that the sample is stationary. Focal adhesions, on the other hand, are dynamic entities that not only evolve over time, but also can undergo translational motion. For instance, focal adhesion velocities in stationary fibroblasts have been reported to be in the range of 100 nm per minute[8]. A temporal resolution below one minute is therefore required to avoid motion blur that would impede detailed observation of this dynamic behavior[9]. However, generating individual PALM images from a smaller number of camera frames in order to increase the temporal resolution, results in less available fluorophore localizations, and therefore decreases the spatial resolution.

* aleksandra.radenovic@epfl.ch; phone +41 21 69 37371; lben.epfl.ch

Single Molecule Spectroscopy and Superresolution Imaging X, edited by Jörg Enderlein, Ingo Gregor, Zygmunt Karol Gryczynski, Rainer Erdmann, Felix Koberling, Proc. of SPIE Vol. 10071, 100710E · © 2017 SPIE · CCC code: 1605-7422/17/$18 · doi: 10.1117/12.2252865

An interesting alternative to PALM is super-resolution optical fluctuation imaging (SOFI), based on a spatio-temporal cumulant analysis of the correlated response of neighboring pixels in a sequence of camera frames[10]. Compared with PALM, this technique tolerates higher fluorophore densities or higher activation rates, resulting in an improved temporal resolution[11]. Additionally, an extension called balanced SOFI (bSOFI) can be used to determine the fluorophore on-time ratio, which allows to estimate of the fluorophore density[12]. In previous work, we investigated the complementarity of PALM and SOFI by applying both techniques to the same sequence of camera frames[13]. PALM was found to give reliable estimates of fluorophore numbers in low-density areas, while SOFI was capable of extracting fluorophore densities in high-density regions. However, it remains unclear to what extent this PALM-SOFI approach is applicable to moving focal adhesions in living cells.

Here, we investigate the complementarity of PALM and SOFI for quantitative imaging in living cells. We perform simulations and demonstrate our approach on live cell data.

2. MATERIALS AND METHODS

2.1 Experiments

The live cell experiments were described in our previous work[13]. Briefly, we used a custom built microscope equipped with a temperature and CO_2 controlled incubator[11]. A 120 mW 405 nm laser (iBeam smart, Toptica) was used for activation, and a 800 mW 532 nm laser (MLL-FN-532, Roithner Lasertechnik) was used for excitation. We used a 60× objective (Apo N 60×, Olympus) with a numerical aperture of 1.49 that allows for TIRF illumination. The fluorescence light was detected by an EMCCD camera (iXon DU-897, Andor), resulting in a 96 nm pixel size.

The mouse embryonic fibroblasts (MEFs) were grown in DMEM supplemented with 10% fetal bovine serum, 1% penicillin-streptomycin, 1% non-essential amino acids, and 1% glutamine, at 37 °C with 5% CO_2. The cells were transfected with 2 µg of the mEos2-paxillin-22 vector using electroporation (Neon Transfection System, Invitrogen). The transfected cells were seeded in a chambered cover slip system (Lab-Tek II Chambered Coverglass System, Thermo Scientific) and grown for around 24 h in cell medium without penicillin-streptomycin.

The living MEFs were imaged in DMEM with a low fluorescence background (FluoroBrite DMEM, Thermo Scientific) at 37 °C with 5% CO_2. Prior to imaging, 100 nm gold nanospheres (C-AU-0.100, Corpuscular) were added to enable drift correction. Excitation of mEos2 was done at 532 nm with ~8.5 mW power, and activation at 405 nm with ~0.6 mW power. The EMCCD camera gain was 150 and the frame exposure time was 10 ms. At least 8000 camera frames per cell were acquired.

2.2 Simulations

The simulations were carried out according to a procedure similar to the one we reported previously[13]. We simulated a square region of 1×1 µm that was randomly filled with single emitters. For each emitter, the number of photons over time was generated, assuming photokinetics similar to mEos2 in our experiments. All emitters were simulated to undergo lateral motion with a constant velocity. A sequence of camera frames was generated, with the intensity of a pixel in a certain frame obtained by integrating the signals from all emitters with a PSF that extends to that pixel in that frame. The number of photo-electrons was simulated by a Poisson distributed random number with an average value equal to the pixel value, multiplied by the camera detection efficiency and added to the camera thermal noise. Camera gain noise and read-out noise were modelled as additive Gaussian noise. We tested several emitter densities (ranging from 100 to 1600 emitters per μm^2), different numbers of camera frames (ranging from 1000 to 5000 frames), and different velocities (ranging from 0 to 1000 nm per minute). For each scenario, we generated 10 sequences.

2.3 PALM data analysis

The PALM analysis was performed as described in our previous work[13]. Localization of the single emitters in the camera frames was done using a custom written algorithm (Matlab, The Mathworks) that was adapted from an earlier published algorithm[14]. First, peaks were identified in each camera frame by applying a filter and an intensity threshold. Subsequently, the peaks were fitted by maximum likelihood estimation of a 2D Gaussian[15]. Drift was corrected in each camera frame by subtracting the average position of the gold nanospheres in that frame. The PALM images were generated by plotting a 2D Gaussian centered on each emitter position with a standard deviation equal to the localization precision. Only localizations with a precision between 0 and 30 nm were used.

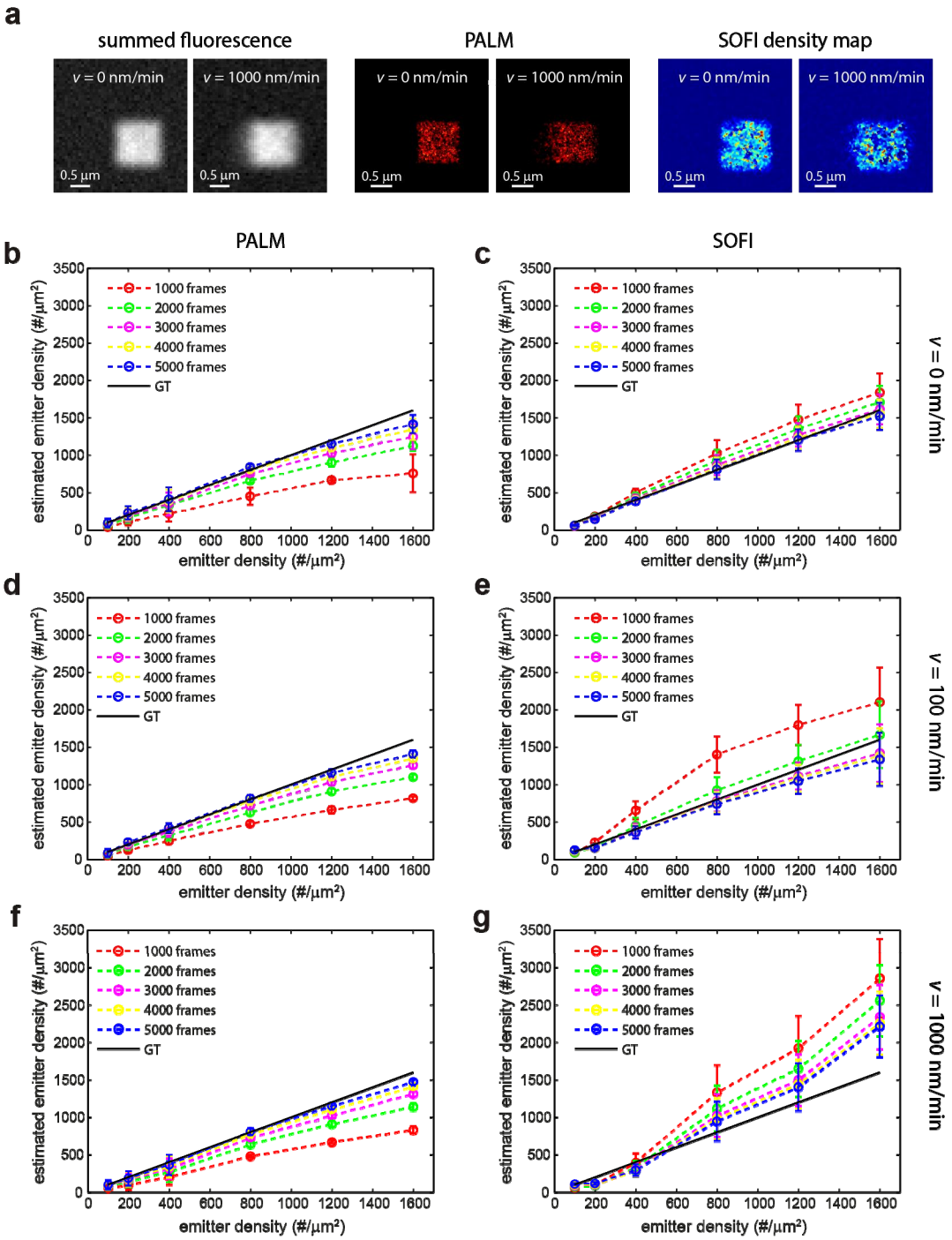

Figure 1. SOFI and PALM based quantitative imaging of simulated data. (a) Summed fluorescence images, PALM images, and SOFI density maps obtained from a simulated sequence of 5000 frames of a 1×1 µm structure randomly filled with emitters at a density of 1600 #/µm^2 and moving with a velocity v equal to 0 or 1000 nm/min. (b-g) The emitter density estimated by (b,d,f) PALM and (c,e,g) SOFI as a function of the ground truth (GT) density for different numbers of simulated frames, and for different velocities v: (b-c) 0 nm/min, (d-e) 100 nm/min, and (f-g) 1000 nm/min. The simulations were repeated 10 times, the error bars represent the standard deviation.

Counting of fluorescent proteins was done by considering all localization pairs with a time interval below a certain threshold t_d as potential blinking events. A second selection was made by applying a distance threshold. To account for the localization precision, the distance threshold was based on the Hellinger distance[13]. We used a value of 0.9 for this threshold. All localization pairs fulfilling these conditions were merged, and the resulting new set of localizations was again evaluated against the same criteria, until no further blinking events could be identified. This procedure was repeated for different values of t_d, and a semi-empirical model[5] was fitted to the protein counts as a function of t_d. The fit was performed for t_d values equal to the first 5 multiples of the camera exposure time[5].

2.4 SOFI data analysis

The SOFI analysis was carried out as reported previously[13]. We used a custom written algorithm (Matlab, The Mathworks) based on the code of our SOFI simulation tool[16] and the bSOFI algorithm[12]. The sequence of camera frames was divided into subsequences of 500 frames each, in order to minimize the influence of photobleaching. Drift was corrected by using the average position of the gold nanospheres to obtain translational motion vectors in between consecutive frames, which were then registered using bilinear interpolation. The linearization step of the bSOFI algorithm was replaced by an adaptive linearization step that allows a more effective use of the dynamic range available in the SOFI images of higher cumulant order[13].

Higher-order SOFI images contain information about the photophysics of the fluorophores, such as their on-time ratio. This information can be used to estimate a map of the fluorophore density, among other fluorophore properties, based on combining SOFI images of different cumulant orders[12]. We used an estimation of the fluorophore density based on the 2nd, 3rd, and 4th order cumulant images[13]. This estimation is done pixel-wise, and is therefore not relevant for image regions which contain only background. For visualization, the linearized bSOFI image was used as a transparency mask to remove these background regions.

3. RESULTS AND DISCUSSION

3.1 Simulations

PALM and SOFI are both capable of quantitative imaging: PALM yields average values of molecular parameters such as the number of fluorophores, while SOFI generates spatial maps of parameters like the fluorophore density. Previously, we found that PALM gives reliable estimates of fluorophore numbers in low-density areas, while SOFI was capable of extracting number densities in high-density regions[13]. However, these quantitative imaging approaches assume that the structure under observation is stationary, while focal adhesions in living cells are known to be dynamic. We therefore performed simulations in order to investigate the effect of lateral motion on the reliability of SOFI based density estimation and PALM based counting.

As explained in the Materials and Methods, and shown in Figure 1a, we simulated 1×1 μm squares that are randomly filled with emitters exhibiting photophysics similar to mEos2. In order to mimic focal adhesion movement, the square structures were simulated to move with a constant velocity of 0, 100, and 1000 nm per minute. The emitter density was chosen between 100 and 1600 emitters per μm^2, and different temporal resolutions were obtained by simulating different frame numbers, ranging between 1000 and 5000. The results of the SOFI based fluorophore density estimation and the PALM based fluorophore counting analysis are shown in Figures 1b-g.

Both SOFI and PALM require at least 3000 frames for good estimates (see Figures 1b-c), placing a limit on the achievable temporal resolution for quantitative imaging (e.g. around 30 s for a typical camera frame rate of 100 Hz). SOFI estimates are insensitive to the emitter density, while PALM increasingly underestimates the emitter count with an increasing emitter density, due to a higher probability of merging localizations of unrelated emitters. On the other hand, the PALM estimates are not much affected by the velocity of the simulated structure (see Figures 1d,f), since the movement between two blinking events, typically separated by a time interval smaller than 1 s, is small enough to be captured by the Hellinger distance criterion which was intended to account for the localization precision (see Materials and Methods). SOFI overestimates the emitter density for increasing velocities (see Figures 1e,g), because the cumulant analysis increasingly involves pixels that are uncorrelated. However, for velocities in the order of 100 nm per minute, which is typical for focal adhesions, the overestimation is acceptable, provided there are a sufficient number of frames.

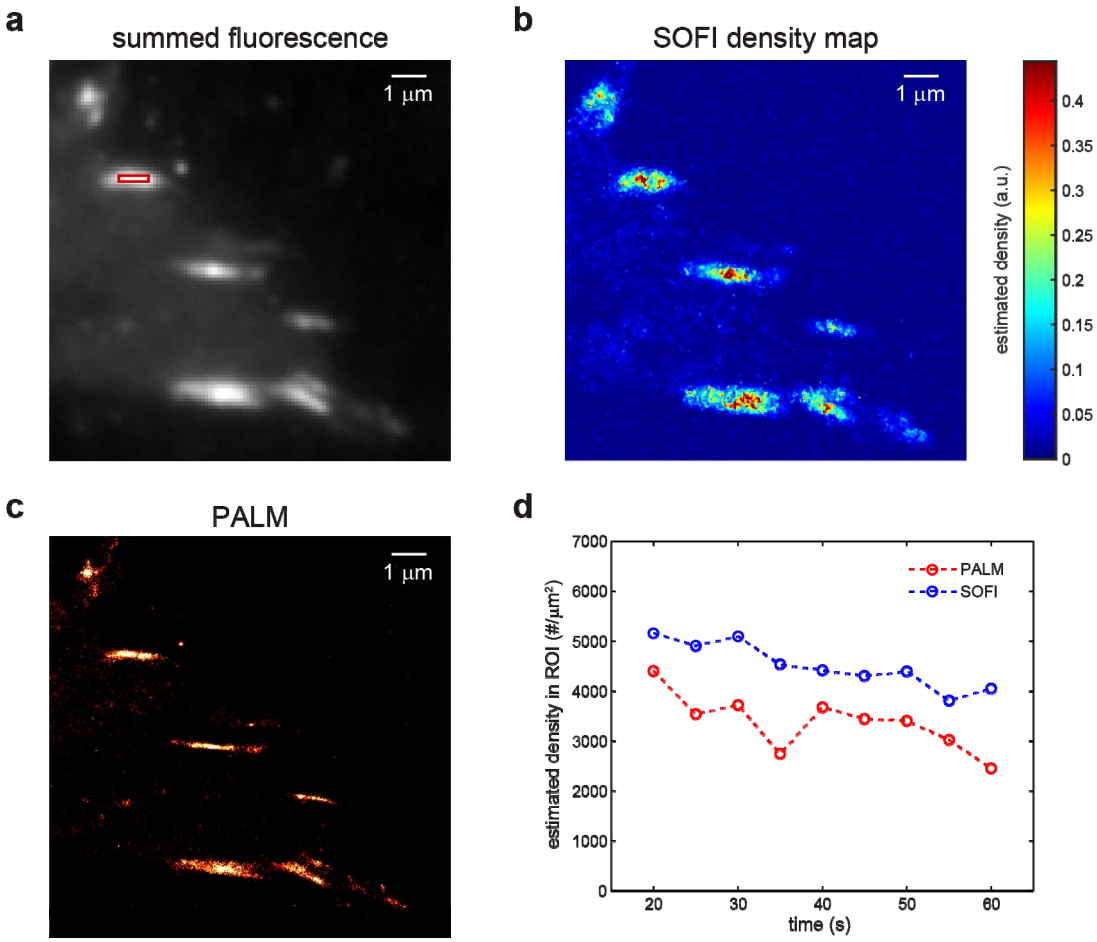

Figure 2. Live cell quantitative imaging with PALM and SOFI. (a) Sum of the first 4000 camera frames in a sequence of 8000 frames of a living MEF cell expressing paxillin labelled with mEos2. (b) SOFI based mEos2 density estimation obtained from the subsequence corresponding to (a). (c) PALM image obtained from the subsequence corresponding to (a). (d) The average mEos2 density in a region of interest (ROI) as a function of time. The ROI was shifted in order to follow the motion of the focal adhesion, the ROI for the first 4000 frames is indicated by the red rectangle in (a). The SOFI based mEos2 density was estimated pixel-wise and then averaged. The PALM based mEos2 density was obtained by dividing the estimated mEos2 number in the ROI with its area. Each point was obtained from a sliding window of 4000 frames, shifted 500 frames between consecutive windows. The frame exposure time was 10 ms, resulting in a 40 s temporal resolution.

3.2 Live cell imaging

After establishing, using simulations, that PALM and SOFI are capable of quantitative imaging of focal adhesions, we applied our PALM-SOFI framework to live cell data, as shown in Figures 2a-c and described in the Materials and Methods. We imaged paxillin labelled with mEos2 in a living MEF cell, and selected a focal adhesion (see the red rectangle in Figure 2a) that was moving with an average speed around 190 nm per minute, as determined previously by kymograph analysis[13]. We found that 4000 frames were required to obtain 4^{th} order SOFI images, which is necessary for fluorophore density estimations. We therefore performed PALM-SOFI based quantitative imaging using a sliding window of 4000 frames through the original sequence of 8000 frames, the results are shown in Figure 2d. PALM counting does not yield densities, but using the same analysis area as for SOFI, an equivalent average mEos2 density can be determined as well. This density falls below the SOFI values, which is in agreement with our simulations. Both PALM and SOFI show that the average mEos2 density decreases over time, likely due to photobleaching.

4. CONCLUSIONS

We performed simulations in order to investigate SOFI based fluorophore density estimation and PALM based fluorophore counting in the context of dynamic structures. The performance of our PALM-SOFI approach is acceptable for fluorophore densities and velocities characteristic of focal adhesions, provided a sufficient number of camera frames are available, typically resulting in a temporal resolution of a couple of tens of seconds. PALM based counting is not sensitive to "high" velocities, but underestimates the fluorophore numbers for large densities, while SOFI based density estimation is not affected by the density, but overestimates densities for "fast" moving structures. This suggests that PALM and SOFI are complementary techniques for quantitative imaging of focal adhesions in living cells, which was demonstrated by determining the average flourophore density in a moving focal adhesion of a living cell.

ACKNOWLEDGEMENTS

The MEF cells were kindly provided by Dr. Luca Scorrano. The mEos2-paxillin-22 vector was kindly provided by Dr. Michael Davidson. H.D. and A.R. acknowledge the support of the Max Planck-EPFL Center for Molecular Nanoscience and Technology. A.R. and T.La. acknowledge the support of the Horizon 2020 project AD Gut (SEFRI 16.0047). We highly appreciate the partial funding by the Swiss National Science Foundation (SNSF, http://www.snf.ch/) under grants 200020-159945 and 205321-138305. T.Lu. acknowledges a SCIEX scholarship (13.183).

REFERENCES

[1] Geiger, B., Spatz, J. P. and Bershadsky, A. D., "Environmental sensing through focal adhesions," Nat. Rev. Mol. Cell Bio. 10(1), 21-33 (2009).
[2] Zaidel-Bar, R., Itzkovitz, S., Ma'ayan, A., Iyengar, R. and Geiger, B., "Functional atlas of the integrin adhesome," Nat. Cell Biol. 9(8), 858-868 (2007).
[3] Tabarin, T., Pageon, S. V., Bach, C. T. T., Lu, Y., O'Neill, G. M., Gooding, J. J. and Gaus, K., "Insights into Adhesion Biology Using Single-Molecule Localization Microscopy," Chemphyschem 15(4), 606-618 (2014).
[4] Annibale, P., Vanni, S., Scarselli, M., Rothlisberger, U. and Radenovic, A., "Identification of clustering artifacts in photoactivated localization microscopy," Nat. Methods 8(7), 527-528 (2011).
[5] Annibale, P., Vanni, S., Scarselli, M., Rothlisberger, U. and Radenovic, A., "Quantitative Photo Activated Localization Microscopy: Unraveling the Effects of Photoblinking," Plos One 6(7), e22678 (2011).
[6] Lee, S. H., Shin, J. Y., Lee, A. and Bustamante, C., "Counting single photoactivatable fluorescent molecules by photoactivated localization microscopy (PALM)," P. Natl. Acad. Sci. USA 109(34), 17436-17441 (2012).
[7] Sengupta, P. and Lippincott-Schwartz, J., "Quantitative analysis of photoactivated localization microscopy (PALM) datasets using pair-correlation analysis," Bioessays 34(5), 396-405 (2012).
[8] Smilenov, L. B., Mikhailov, A., Pelham, R. J., Marcantonio, E. E. and Gundersen, G. G., "Focal adhesion motility revealed in stationary fibroblasts," Science 286(5442), 1172-1174 (1999).
[9] Shroff, H., Galbraith, C. G., Galbraith, J. A. and Betzig, E., "Live-cell photoactivated localization microscopy of nanoscale adhesion dynamics," Nat. Methods 5(5), 417-423 (2008).
[10] Dertinger, T., Colyer, R., Iyer, G., Weiss, S. and Enderlein, J., "Fast, background-free, 3D super-resolution optical fluctuation imaging (SOFI)," P. Natl. Acad. Sci. USA 106(52), 22287-22292 (2009).
[11] Geissbuehler, S., Sharipov, A., Godinat, A., Bocchio, N. L., Sandoz, P. A., Huss, A., Jensen, N. A., Jakobs, S., Enderlein, J., van der Goot, F. G., Dubikovskaya, E. A., Lasser, T. and Leutenegger, M., "Live-cell multiplane three-dimensional super-resolution optical fluctuation imaging," Nat. Commun. 5, 5830 (2014).
[12] Geissbuehler, S., Bocchio, N. L., Dellagiacoma, C., Berclaz, C., Leutenegger, M. and Lasser, T., "Mapping molecular statistics with balanced super-resolution optical fluctuation imaging (bSOFI)," Optical Nanoscopy 1, 4 (2012).
[13] Deschout, H., Lukes, T., Sharipov, A., Szlag, D., Feletti, L., Vandenberg, W., Dedecker, P., Hofkens, J., Leutenegger, M., Lasser, T. and Radenovic, A., "Complementarity of PALM and SOFI for super-resolution live-cell imaging of focal adhesions," Nat. Commun. 7, 13693 (2016).

[14] Betzig, E., Patterson, G. H., Sougrat, R., Lindwasser, O. W., Olenych, S., Bonifacino, J. S., Davidson, M. W., Lippincott-Schwartz, J. and Hess, H. F., "Imaging intracellular fluorescent proteins at nanometer resolution," Science 313(5793), 1642-1645 (2006).
[15] Mortensen, K. I., Churchman, L. S., Spudich, J. A. and Flyvbjerg, H., "Optimized localization analysis for single-molecule tracking and super-resolution microscopy," Nat. Methods 7(5), 377-381 (2010).
[16] Girsault, A., Lukes, T., Sharipov, A., Geissbuehler, S., Leutenegger, M., Vandenberg, W., Dedecker, P., Hofkens, J. and Lasser, T., "SOFI Simulation Tool: A Software Package for Simulating and Testing Super-Resolution Optical Fluctuation Imaging," Plos One 11(9), e0161602 (2016).